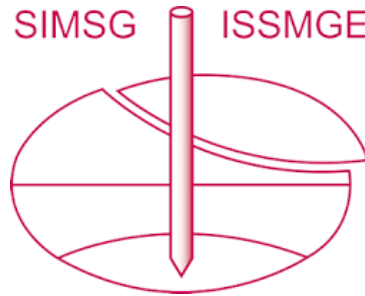


INTERNATIONAL SOCIETY FOR SOIL MECHANICS AND GEOTECHNICAL ENGINEERING



This paper was downloaded from the Online Library of the International Society for Soil Mechanics and Geotechnical Engineering (ISSMGE). The library is available here:

<https://www.issmge.org/publications/online-library>

This is an open-access database that archives thousands of papers published under the Auspices of the ISSMGE and maintained by the Innovation and Development Committee of ISSMGE.

The paper was published in the proceedings of the 11th International Symposium on Field Monitoring in Geomechanics and was edited by Dr. Andrew M. Ridley. The symposium was held in London, United Kingdom, 4-7 September 2022.

Multi-source monitoring data and numerical analyses for the assessment of settlements affecting built-up areas in variable soil conditions

Alfonso PROSPERI¹, Gianfranco NICODEMO², Mandy KORFF^{1,3}, Dario PEDUTO²

¹ Delft University of Technology, Faculty of Civil Engineering and Geosciences, Delft, The Netherlands

² University of Salerno, Department of Civil Engineering, Fisciano (SA), Italy

³ Deltares, Delft, The Netherlands

Corresponding author: Gianfranco Nicodemo (gnicodemo@unisa.it)

Abstract

This paper presents an integrated analysis based on the use of multi-source wide-area datasets consisting of hydro-mechanical properties of geomaterials, in-situ investigations/measurements (e.g. groundwater levels in wells) and innovative space-borne data (i.e. DInSAR techniques) to support numerical analyses aimed at assessing and predicting the settlements affecting built-up areas in variable soil conditions. To this aim, an expeditious procedure was developed and tested with reference to a district in Rotterdam City (The Netherlands) affected by subsidence phenomena due to the presence of heterogeneous settling strata mainly composed by peat and organic soils. The results obtained allowed investigating the role of predisposing factors of the settlement occurrence and assessing the induced damage on buildings. Considering the widespread diffusion of such geohazards, the followed procedure could help the in-charge authorities to carry out activities at urban scale aimed at identifying the areas most affected by subsidence risk and to select the most suitable and sustainable mitigation strategies.

Keywords: Multi-source monitoring, Soil variability, Settlements, Built heritage, Numerical modelling

1 Introduction

Land subsidence is a well-known phenomenon associated with the gradual sinking of the ground surface affecting many deltaic areas worldwide. The magnitude, rates and the distribution of subsidence-related displacements are highly influenced by the characteristics of the subsurface, the ground water regime as well as the nature of the triggering phenomena (linked to either natural or anthropogenic processes). An example is the western coastal-deltaic plain of the Netherlands, in which the presence of unconsolidated clayey and peat-rich shallow soil strata (namely “soft soils”) predisposes to the occurrence of natural subsidence. Thus, structures and infrastructure networks are exposed to settlement-induced damage and an increase of the flooding risk and seawater intrusions.

Therefore, the monitoring of land subsidence represents a challenging yet key task in the performance control of the exposed (infra)structure. In this regard, measurements acquired using both conventional and innovative techniques can help in assessing and predicting the subsidence occurrence and magnitude over the affected urban areas. Nevertheless, conventional monitoring techniques can be far too demanding and unaffordable when the study involve large areas (e.g. neighbourhood, city, region or country). In the above-mentioned cases, innovative and non-invasive remote sensing techniques such as images acquired by spaceborne synthetic aperture radar (SAR) and processed via differential interferometric techniques (DInSAR) represent a valuable alternative, providing displacement measurements on the regional/urban scale (Peduto et al., 2019). These latter, complemented with available ancillary information retrieved by national/regional/municipal datasets and compared with results of numerical simulations, can valuably support the full comprehension of subsidence phenomena, and in turn, the prediction of the induced consequences in urban areas.

Within the framework of subsidence risk mitigation, the paper synthesizes some results of a wider ongoing research project in which multi-source monitoring data feed numerical analyses to assess and predict subsidence-related settlements in built-up areas. For this purpose, the wide-area information about the subsurface variability, the typical loading (transferred by structures) conditions, the water table drawdown measurements and DInSAR-derived settlements were collected and analysed over the selected study area. This allowed identifying 225 typical hydro-geomechanical-loading (HGL) scenarios that were then implemented in numerical analyses to identify the “most critical” conditions in terms of settlement occurrences and differential settlements affecting the buildings. The results allowed *i)* highlighting the role played by the main

predisposing/triggering factor(s) in the occurrence, magnitude, and spatial distribution of settlements and ii) assessing the building damage using available empirical fragility curves.

2. Methodology

The procedure followed in this study consists of three main phases (Fig. 1). In Phase I, multi-source and spatially-distributed information including: i) displacement monitoring data retrieved from innovative DInSAR techniques, ii) hydro-geo-mechanical properties of the recurrent soil layers along with their stratigraphic assets, iii) ground water level measurements in wells, and iv) building features useful to derive typical loading conditions, were collected over the study area. The above-mentioned datasets were preliminary homogenised and examined at the district scale for their use in the Phase II (Fig. 1). This latter was aimed at identifying “typified” Hydro-Geomechanical-Loading (H_iG_iL_i) scenarios, which were implemented in numerical simulations to assess settlements affecting the selected built-up area.

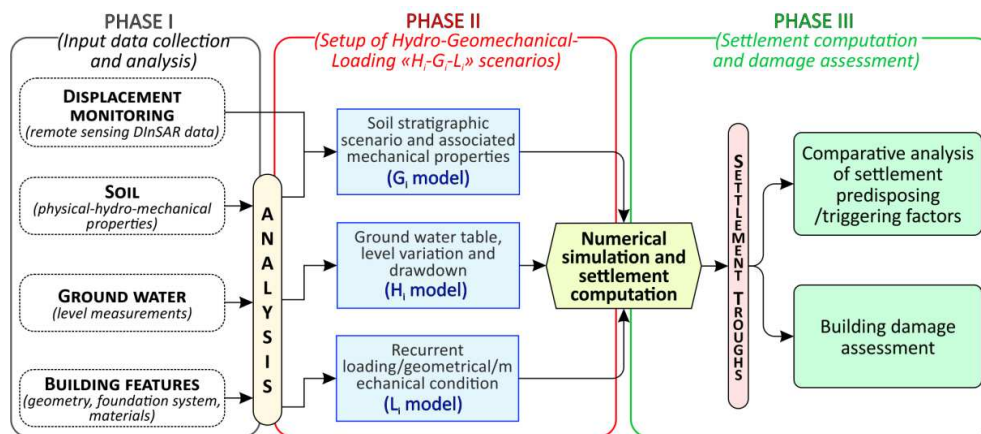


Figure 1: Flowchart of the followed procedure (modified from Peduto et al., 2022).

To this end, the variability of the soil types and layer thicknesses extracted from the investigated boreholes covering the study area were first analysed. This allowed obtaining the mean and standard deviation values of the cumulative soil thickness of the examined subsurface. Then, considering that the ground displacements associated with the presence of “soft soil” strata can be highly variable depending on their cumulative thickness and compressibility as well as their spatial distribution, geological cross-sections were drawn across the boreholes to derive typified subsurface stratigraphy. Additionally, the relationship between the soft soil cumulative thickness along selected sections across the boreholes and the settlement magnitude on the ground (i.e. in free-field conditions) was investigated. Accordingly, vertical DInSAR-derived settlements at the ground level were compared with the cumulative thickness of “soft soil” extracted by the boreholes. Similarly, the DInSAR-derived cumulative settlements measured on top of the buildings were compared with the settlements computed for built locations by means of simplified mono-dimensional numerical analyses conducted for each borehole considering the loads transferred by the buildings. The numerical simulations were carried out with Plaxis2D software considering a 5-year time interval, which is equal to the measurement period of DInSAR-derived cumulative settlements (years 2009–2014). The above comparison allowed defining the typical soil stratigraphic scenarios and fixing their mechanical parameters that are jointly referred as geomechanical (G_i) model (Fig. 1). As for the groundwater level, including its variation and the drawdown, hydro (H_i) models were set up based on the analysis of time series acquired from the available piezometric wells that, together with the observed water head variation, allowed defining the time-dependent lowering functions used in the numerical simulations. The typical building loading conditions (L_i) were established considering a model structure based on the analysis of the main building features that should represent the most common building geometries and, in turn, loading conditions in the district area. Finite element analyses conducted using Plaxis2D software were carried out for each defined HGL scenario by combining the geometry of the loading conditions (L_i), the stratigraphic assets and the physical–hydro-mechanical properties of the soil types (G_i), and the groundwater level (H_i) considering the lowering of the water table as the triggering factor for settlement occurrence. For this purpose, fully coupled flow-deformation analyses were carried out for the

consolidation process. In particular, soft soil creep model (SSC) was assigned to peat, clay, and silt soils; while a Mohr-Coulomb (MC) criterion was assigned to the sand.

In Phase III (Fig. 1), the results of the numerical simulation in terms of settlement troughs and subsidence-related intensity (SRI) parameter (i.e., differential settlements) recorded in correspondence of the building footprint were firstly used to study the role played by the different factors (i.e., stratigraphy, water drawdown, and loading conditions) contributing to building settlements and then to assess the building damages.

3. Case study and available datasets

The residential neighbourhood selected for the analyses was Bloemhof, located in Rotterdam City in the Rhine-Meuse Delta area (Fig. 2a). Rotterdam City is a typical example of a delta city resting on soft soils. Indeed, its subsurface is mainly composed by shallow Holocene peaty, clayey and sandy layers (Fig. 2b), down to the depth of 20 meters, overlapped with a Pleistocene layer of sand (de Doelder and Hannink, 2015).

Subsidence is a widespread problem in the whole urban area that has been recurrently causing social unease and high costs due to repair and adaptation works for damaged buildings and the infrastructure networks. Particularly, the building stock in Bloemhof mostly consists of 2–3 floored masonry buildings (typical row houses) dating back to the 1920s, resting on either shallow and deep foundations. These buildings have been reported to be exposed to subsidence phenomena (Ghodsvali, 2018).

The available “GeoTOP model” (www.dinoloket.nl) provided the subsurface information for this study. The model discretize the entire Dutch territory in million of voxels, each measuring 100 × 100 × 0.5 m (height × width × depth), down to 50 meters below the ground surface. Each voxel provide the information of the most probable lithostratigraphy and lithological classes, resulting from the collection and geostatistical analysis of boreholes and field tests (Stafleu et al., 2011). In this study, the physical and mechanical properties of the soils types (Table 1) were retrieved from the Dutch standards (NEN 9997-1+C2 2017).

Soil type	Physical and mechanical parameters											
	γ	γ_{sat}	$C_c/(1+e_0)$	E'	ϕ'	c'	c_u	k	λ^*	k^*	μ^*	OCR
	[kN/m ³]	[kN/m ³]	[-]	[MPa]	[°]	[kPa]	[kPa]	[m/s]	[-]	[-]	[-]	[-]
Anthropogenic soil	18	20	0.0038	45.0	32.5	0.0	-	1.16×10^{-5}	-	-	-	1.00
Holocene sand	18	20	0.0038	45.0	32.5	0.0	-	1.16×10^{-5}	-	-	-	1.00
Pleistocene sand	19	21	0.0023	75.0	35.0	0.0	-	1.16×10^{-5}	-	-	-	1.00
Silt	20	20	0.092	5.00	27.5	1.0	10	1.08×10^{-7}	0.0400	0.0080	0.0016	1.90
Clay	17	17	0.1533	2.00	17.5	5.0	50	3.41×10^{-10}	0.0667	0.0133	0.0027	1.90
Organic soil	12	13	0.3067	0.50	15.0	15.0	2.5	1.77×10^{-7}	0.1333	0.0267	0.0053	1.90

Table 1: Physical and mechanical properties of soil types in the study area: unsaturated unit weight γ ; saturated unit weight γ_{sat} ; compression ratio, $C_c/(1+e_0)$; effective Young's modulus, E' ; friction angle, ϕ' ; effective cohesion, c' ; undrained shear strength, c_u ; hydraulic conductivity, k ; modified compression index, λ^* ; modified swelling index, k^* ; modified creep index μ^* ; over-consolidation ratio OCR; (from Dutch standards, NEN 9997-1+C2 2017).

Groundwater monitoring network with water-head level measurements monthly acquired (Gemeente Rotterdam, 2020) are freely available from approximately 2000 wells (30 of which are still operative and located over the study area, Fig. 2a). These measurements indicates a water head ranging between -2.50 m and -1.50 m from the NAP (Normaal Amsterdams Peil) level.

As for displacement measurements, data at both ground (e.g., free-field condition, Fig. 2c) level and on top of building (at the roof level, Fig. 2d), derived by processing 285 SAR images (acquired on ascending and descending orbits from 2009 to 2014 by the TerraSAR-X (TSX) satellite constellation) via Advanced Differential Interferometric (A-DInSAR), are available. The data show that free-field displacement rates exceed 5mm/year in many portions of the analysed district (Fig. 2c), whereas velocity values recorded on top of the buildings are rarely higher than 3 mm/year (Fig. 2d).

Finally, available probabilistic relationships between the differential settlement (SRI parameter) and building damage severity levels in the form of empirical fragility curves derived ad hoc for 180 settlement-affected

Dutch masonry buildings on shallow foundations (Peduto et al. 2019), were used for the damage assessment at the district scale.

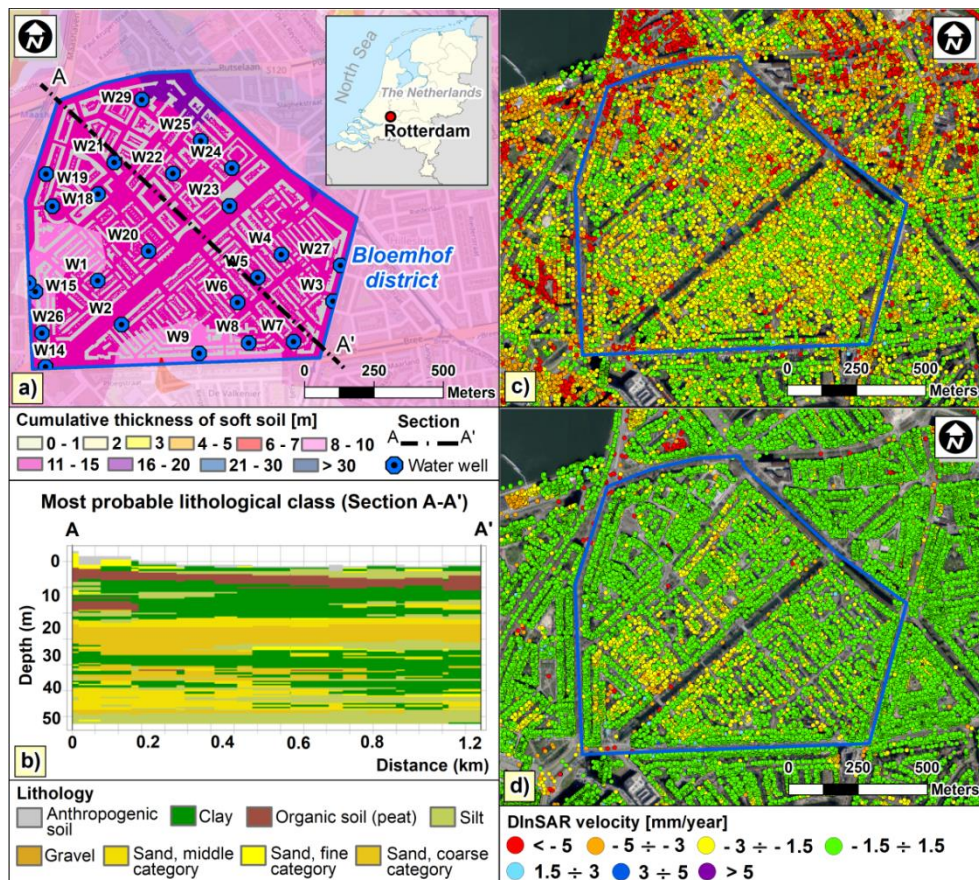


Figure 2: Bloemhof study area: a) cumulative thickness of soft soils (organic and clayey) with water wells for groundwater measurements and b) geological cross-section along the A–A' profile sketched in panel a) (extracted from the portal of the Geological Survey of the Netherlands — DINOloket, www.dinoloket.nl); maps of TSX DInSAR data on ascending and descending orbit at the ground level c) and on the top of buildings d).

4. Results

Following the proposed procedure (Fig. 1), the collected information at the district scale in the Phase I allowed building a multi-source dataset to define, in the Phase II, the equivalent geotechnical and loading models representing the “typified” HGL scenarios. Specifically, starting from the stratigraphy of the 13 selected boreholes (Fig. 3a) the mean and standard deviation of the thickness values of peaty, clayey, silty, and sandy soil layers were calculated. From the comparison between the cross-sections and the DInSAR-derived cumulative settlement magnitude in free-field, the influence of spatial variability of soil layers was studied.

For instance, looking a generic sample section across the B6–B1 boreholes (Fig. 3b), it can be observed that the soft soil (i.e. peat and clay), silt, and sand cumulative thickness did not show significant variations along the cross-section; nevertheless, a variation in the cumulative settlement profile is observable in borehole B6.

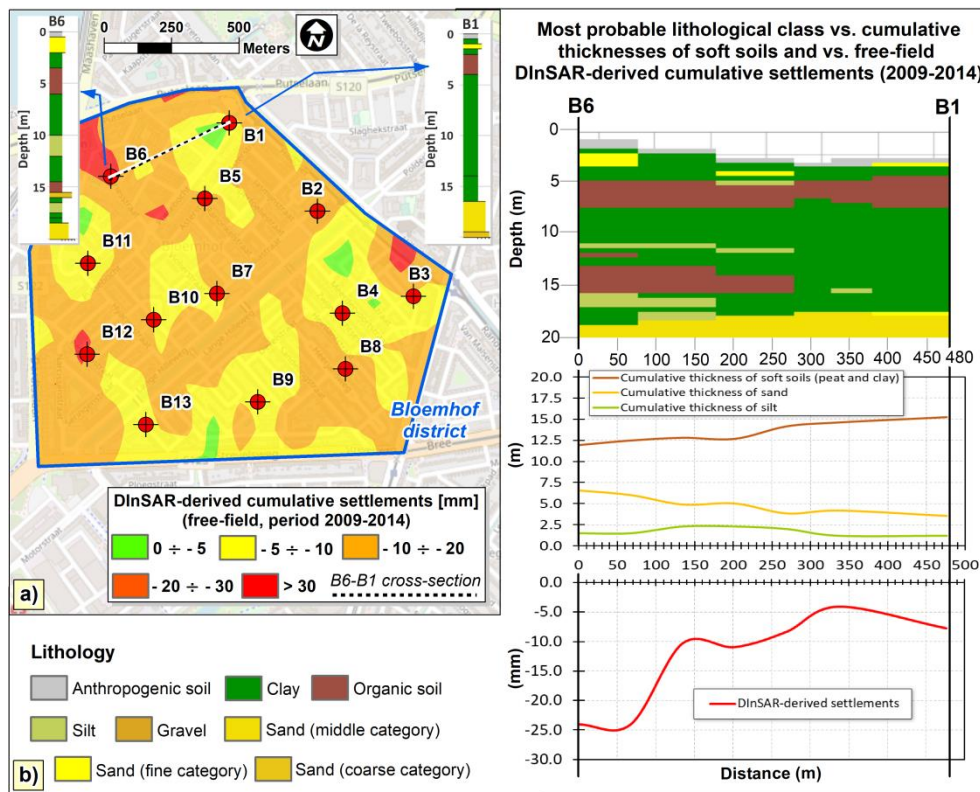


Figure 3: a) spatial distribution of DInSAR-derived cumulative settlements at the ground level with position of the 13 considered boreholes; b) correlation between the geolithological cross-section (boreholes B6–B1) and the cumulative thicknesses of soft soils vs. DInSAR-derived settlements (modified from Peduto et al., 2022).

Therefore, the highest recorded settlements were not only the results of the mutual soil thickness (e.g., in borehole B6 there is an increase in peat and a decrease in clay thickness) along the section, but also of the stratigraphical asset of the soil layer (e.g., shallower organic soil strata can be more influenced by a drawdown of the water table, leading to higher settlements). Accordingly, the thickness and slope of the soil layers under the loading area (building footprint), as well as organic soil inclusions were considered in the definition of the most common geostatigraphic (G_i) scenarios present in the study area.

Five stratigraphic conditions (Fig. 4) were defined based on previous observations; the physical–mechanical soil parameters (see Table 1) were assigned considering also an expeditious validation test comparing the DInSAR-measured settlements on top of the buildings (Fig. 2d) with the settlements computed via simplified mono-dimensional analyses for each investigated borehole (Fig. 4a) as described in the methodology section. As for the water table levels (H_i), in addition to the case of a constant water table at a depth of 1.50 m (H₁), two types of time-dependent drawdowns were defined by using the flow function in Plaxis2D software. In particular, both a linear drawdown (H₂–H₅ conditions) in the time interval of the analysis (30 years) and an immediate drawdown were considered (H₆–H₉ conditions). For each flow function, four water-head variations were assigned, starting from the original level of –1.50 m (–0.25, –0.50, –0.75, –1.00 m), thus modelling eight water table variations (H₂–H₉ conditions; see Fig. 4).

With respect to the building loadings (L_i), five different loading conditions (L₁: symmetrical case; L₂ and L₃: asymmetry in openings; L₄ and L₅: asymmetry in height, Fig. 4) were considered to represent the most common building geometries (i.e., differences in openings or height) with shallow foundation and, in turn, loading conditions (resulting in asymmetric loads) retrieved over the district area.

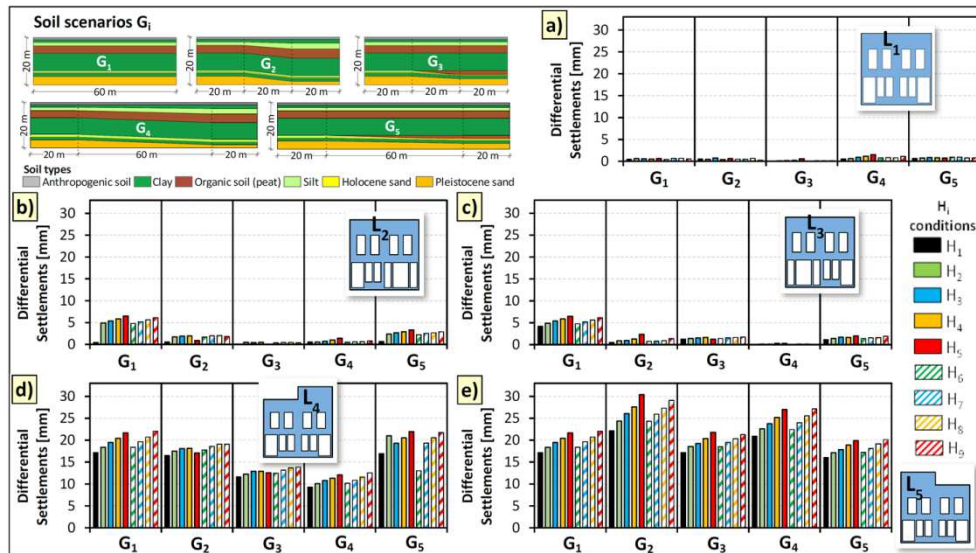


Figure 4: Computed differential settlements by numerical analysis for each typified ($H_iG_iL_i$) scenario: a) L_1 , b) L_2 , c) L_3 , d) L_4 , and f) L_5 loading conditions (modified from Peduto et al., 2022).

According to the assumptions presented in the Methodology chapter, 225 numerical analyses were performed with PLAXIS2D software considering the combination of the water table (H_i), the geostratigraphic (G_i) setting and loading (L_i) conditions as the “typified” $H_iG_iL_i$ scenarios.

For each $H_iG_iL_i$ combination, the maximum differential settlement was calculated as the difference in the vertical settlement between the side points of the building’s footprint. A comprehensive comparison of the obtained results for the 225 analysed scenarios over 30 years is synthesised in the histograms shown in Figure 4, in which, for each G_i and L_i condition, the computed differential settlements are plotted according to the different H_i (H_1 – H_9) conditions.

The results of numerical simulation highlight that the magnitude of differential settlements affecting the building footprint are influenced by predisposing/triggering factors. Indeed, for a given soil scenario G_i the differential settlement intensity increases with the higher values of the water-head variation for both linear and immediate drawdowns. Moreover, the loading L_i conditions significantly affect the results, as highlighted by the asymmetrical loadings (L_4 and L_5 ; see Figs. 4d and 4e) that record higher differential settlement values than the other conditions (L_1 – L_3 ; see Figs. 4a, 4b, and 4c). Moreover, the heterogeneity of the soil jointly with the transferred load (in particular for asymmetrical structure) can lead to higher values of differential settlements. This confirms the usefulness of assuming inclined soil layers rather than horizontal layers in the half-space (Fig. 4), as in the classical approach.

The computed differential settlements were used to assess the damage that buildings may experience using available empirical fragility curves for masonry buildings on shallow foundations. Particularly, by entering the curves with the computed differential settlement over 30 years, it is possible to retrieve, for each scenario, the probability for each building to reach or exceed a certain damage severity level D_i (i.e., D_1 = very slight, D_2 = slight, D_3 = moderate damage; see Peduto et al., 2019), which was ranked according to the classification of Burland et al. (1977).

Figure 5 shows an example for the L_5 loading condition resting on G_2 soil scenarios, which the previous results identified as inducing the highest differential settlements leading to higher probability of more severe damage. Indeed, visible damages in terms of cracks on the building façades were recorded in Bloemhof district (an example is show in Fig. 5). This highlights as the combined use of ad hoc fragility curves with the numerically computed differential settlement would allow to predict – considering the different H_i , G_i and L_i conditions – the expected damage level (D_i) for all buildings resting on shallow foundations over the Bloemhof district in a pre-fixed time interval (Peduto et al., 2022).

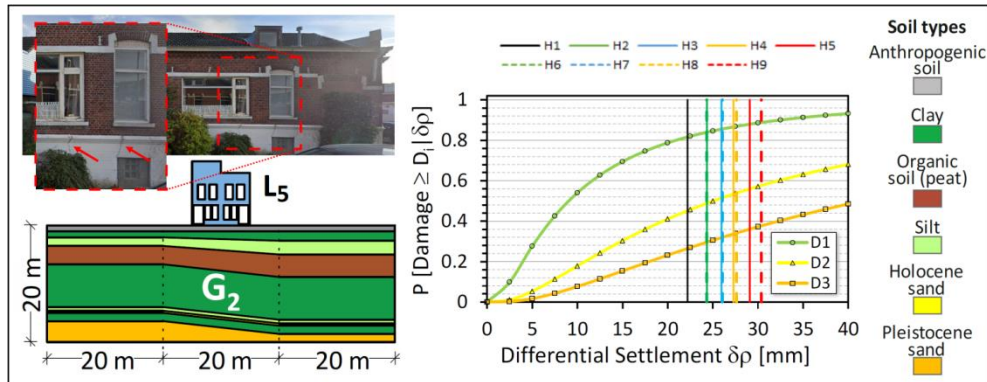


Figure 5: Building damage assessment undergoing differential settlements using empirical fragility curves proposed by Peduto et al. (2019). An example for the L_5 loading condition resting on G_2 soil scenarios for the different H_i water level variations with some photos of cracks recorded on a building façades in Bloemhof.

4. Conclusions

The paper presented the results of the combined use of multi-source monitoring data and numerical analyses to assess and predict the subsidence-related settlements affecting built-up areas. The analyses of 225 simplified hydro-geomechanical-loading (HGL) scenarios allowed investigating the role of three main factors (i.e. soil heterogeneity, loading conditions, and groundwater variations) on both the magnitude and spatial distribution of settlements in the study area as well as assessing the damage of building undergoing differential settlements. Indeed, the outcomes of the numerical simulations, compared with the monitoring data, can help to achieve a better understating of subsidence-related criticalities in urban areas. Therein, the presented procedure could represent an efficient way for both professionals, researchers and territorial agencies to address proper mitigation strategies by efficiently prioritizing those areas affected by subsidence-related problems.

Acknowledgements

The authors gratefully acknowledge Sky-Geo Netherlands B.V. for supplying the DInSAR data.

References

- Burland, J. B., Broms, B. B., De Mello, V. F. (1977). Behaviour of foundations and structures. SOA report. *Proc. of the 9th Int. Conf. on Soil Mechanics and Foundation Engineering*, Tokyo, Japan. Vol. 2. pp. 495–546.
- de Doelder, B. and Hannink, G. (2015). Risk Management of Groundwater During The Reconstruction of the Rotterdam Central area. *Geotechnical Safety and Risk V*, IOS Press, pp. 583-589.
- Gemeente Rotterdam. (2020). Gis Rotterdam [online]. Available at: <https://www.gis.rotterdam.nl/gisweb2/default.aspx>
- Ghodsvali, M. (2018). *3D modelling of underground space for urban planning and management-providing basic planning insight*. M.Sc. Thesis, University of Twente, pp. 1-120. <http://purl.utwente.nl/essays/83764>
- NEN 9997-1+C2. (2017). Geotechnisch ontwerp van constructies - Deel 1: Algemene regels (*Geotechnical design of structures - Part 1: General rules*). ICS Code 93.020.
- Peduto, D., Korff, M., Nicodemo, G., Marchese, A., Ferlisi, S. (2019). Empirical fragility curves for settlement-affected buildings: analysis of different intensity parameters for seven hundred masonry buildings in the Netherlands. *Soils and Foundations*, 59(2): 380–397.
- Peduto, D., Prosperi, A., Nicodemo, G., Korff, M. (2012). District-scale numerical analysis of settlements related to groundwater lowering in variable soil conditions. *Canadian Geotechnical Journal*. <https://doi.org/10.1139/cgj-2021-0041>
- Stafleu, J., Maljers, D., Gunnink, J., Menkovic, A., Busschers, F. (2011). 3D modelling of the shallow subsurface of Zeeland, the Netherlands. *Netherlands Journal of Geosciences*, 90(4), 293-310.